Polarimetric attenuation correction and rainfall estimation at C band for an extreme rain event

J-Y. Gu
Department of Environmental and Atmospheric Sciences,
Pukyong National University, Busan, South Korea

A. Ryzhkov
Cooperative Institute for Mesoscale Meteorological Studies,
University of Oklahoma, USA

P. Zhang
Cooperative Institute for Mesoscale Meteorological Studies,
University of Oklahoma, USA

P. Neilley
WSI Corporation and Enterprise Electronics Corporation (EEC), USA

M. Knight
WSI Corporation and Enterprise Electronics Corporation (EEC), USA

B. Wolf
University of Valparaiso, USA

D.-I. Lee
Department of Environmental and Atmospheric Sciences,
Pukyong National University, Busan, South Korea

To be submitted to the Journal of Applied Meteorology and Climatology

1. Introduction

S-band weather radars are primarily utilized for the observations of severe storms. The major reason for this is that shorter-wavelength radars may experience significant attenuation in heavy precipitation. A long-standing problem of attenuation correction at shorter radar wavelengths can be efficiently resolved if the radar has dual-polarization capability. In addition, dual-polarization radars possess unique classification potential as

opposed to the conventional single-polarization Doppler radars which do not distinguish between different hydrometeor types. Data quality issues with conventional radar such as radar miscalibration, partial beam blockage, contamination from nonmeteorological echo can be overwhelming and difficult to address, whereas polarimetry offers very efficient and elegant ways to improve data quality. Finally, polarimetric radar provides significant improvement in the accuracy of rainfall estimation.

The purpose of this study is to illustrate mentioned advantages of polarimetric radar measurements at C band for the case of severe thunderstorm in the Chicago metropolitan area which made headlines in mass media because of its severity and number people and businesses affected. The storm produced tremendous amount of rain in a short period of time and caused record attenuation of the C-band radar signal in excess of 40 dB which presents huge challenge for the attenuation correction algorithm.

The WSR-88D radars which comprise the existing network of the US National Weather Service (NWS) operate at S band and are less prone to attenuation than shorter-wavelength radars. According to the NWS plans, single-polarization WSR-88D radars will be retrofitted in the next few years by adding polarimetric capability and, in the long run, may be complemented by C-band and X-band polarimetric radars for better areal coverage. Note that the bulk of weather radars utilized by the US Federal Aviation Administration (FAA) in the terminal areas of airports operates at C band. Television companies also use C-band Doppler radars, some of which already have polarimetric diversity. Hence, it is important to investigate and demonstrate abilities of such radars to quantitatively assess characteristics of severe storms in the presence of strong attenuation. Polarimetric radar measurements at C band are rare in USA (as opposed to Europe, Canada, Australia, and some Asian countries) and the presented observational study is one of the first in the American continent.

Attenuation correction in heavy rain is one of the main focuses of this study. Polarimetric methods for attenuation correction of radar reflectivity Z and differential reflectivity Z_{DR} utilize measurements of differential phase Φ_{DP} which is immune to attenuation (Bringi and Chandrasekar 2001). Simplified versions of the attenuation correction techniques assume that the coefficients of proportionality α and β between the Z and Z_{DR} biases and Φ_{DP} do not vary much (Bringi et al. 1990). However, at C band, these are highly variable in convective cells containing large raindrops and hail due to effects of resonance scattering (Carey et al. 2000; Bringi et al. 2001; Ryzhkov et al. 2006, 2007, Tabary et al. 2008, Vulpiani et al. 2008). More sophisticated schemes for attenuation correction attempt to estimate the coefficients α and β in such "hotspot" cells using additional constraints. In this paper, we develop one of such schemes and test it on the data collected during an extreme rain event in the Chicago metropolitan area observed by the C-band Sidpol polarimetric radar built by the Enterprise Electronics Corporation (EEC) and owned by the University of Valparaiso.

Results of attenuation correction are validated using self-consistency between radar polarimetric variables and comparisons with the measurements from nearby WSR-88D S-band radar which didn't experience much attenuation in the storm. Additionally, we evaluate the quality of rainfall estimation in this storm using available rain gage data.

2. Description of the storm and radar dataset

a. Overview of the storm

Synoptic conditions on the day of August 4, 2008 were very favorable for development of deep convection in the US Midwest. Arctic high pressure stretched from Canada to the middle of US and a stationary front associated with this high extended to Illinois and Indiana. At the same time, the area of high pressure over the southeastern US allowed moisture transportation from the Gulf of Mexico. The moisture was brought by

the hurricane "Edouard" which hit the coast of Texas and Louisiana at that time. The sounding data obtained from the Lincoln observation site (250 km west from the Sidpol radar) indicated strong possibility of violent thunderstorms. The corresponding CAPE value was 7034 Jkg^{-1} and associated Lifted Index was -13.

The thunderstorm hit the Chicago Metropolitan area at about 00 UTC on 2008/08/05 producing damaging wind and torrential rain. Four tornadoes struck the Chicago area and severe thunderstorms pummeled the surrounding region. Thousands of travelers at the O'Hare Airport and fans at the Wrigley field were evacuated. Many homes and businesses were damaged as a result of the storm. Wind gusts sped up to over 90 miles an hour and one fatality was reported in northwest Indiana from a falling tree. No hail was reported on the ground during this storm.

b. Radar data processing and quality control

The storm was in the coverage area of the C-band Sidpol radar for at least 2 hours before the leading edge of the squall line passed over the radar site at about 0149 UTC on August 5th, 2008 and radar data recording was interrupted due to the lightning strike. Strom localization between Sidpol radar and the KLOT WSR-88D radar provided excellent opportunity to compare radar observations at C and S bands (Fig. 1).

Sidpol radar measured horizontal reflectivity (Z), differential reflectivity (Z_{DR}), differential propagation phase (Φ_{DP}), and cross-correlation coefficient (ϱ_{hv}) with radial resolution of 0.125 km and azimuthal resolution of about 0.83° within the range 180 km from the radar. Simple radial smoothing via box-car averaging is performed with a 1 km window for Z, Z_{DR} and ϱ_{hv}.

Extremely high values of Φ_{DP} have been measured in this storm. An example of the radial profile of measured Φ_{DP} is shown in Fig. 2a. The recorded differential phase exhibits double folding and needs to be dealiased before the estimation of its radial derivative, specific differential phase K_{DP}, can be performed. A three-step procedure was utilized for the Φ_{DP} unfolding and processing. This implies downward shifting of differential phase as shown in Fig. 2b, elimination of the Φ_{DP} jump caused by aliasing, and editing and smoothing of Φ_{DP} using the measurements of ϱ_{hv} (Fig. 2c).

Absolute calibration of Z and Z_{DR} was checked using the radar data. The consistency between Z and K_{DP} in rain was utilized to evaluate absolute calibration of Z. General principles of the polarimetric consistency checks are described by Gorgucci et al. (1992), Goddard et al. (1994), Ryzhkov et al. (2005) among others. At C band, it is expected that Z and K_{DP} are consistent for moderate-to-heavy rain within the radar reflectivity interval between 40 and 50 dBZ.

Examination of the measured Z_{DR} in dry aggregated snow above the melting layer in a stratiform part of the storm and analysis of the $Z - Z_{DR}$ scatterplots in rain for $Z < 40$ dBZ were utilized to unbias the measurements of Z_{DR}. According to Ryzhkov et al. (2005), intrinsic Z_{DR} in dry aggregated snow should be within the range 0.1 – 0.2 dB. The observed scatterplot of Z_{DR} versus Z in rain has to be in agreement with the one obtained from theoretical simulations at C band (see Section 3).

Although Z_{DR} and ϱ_{hv} are supposed to be corrected for noise in modern radar data processors, additional check based on the analysis of polarimetric data is highly recommended because noise powers in orthogonal receiver channels may not be carefully monitored. Both polarimetric variables become biased by noise if signal-to-noise ratio (SNR) drops below 20 – 25 dB. Estimating of Z_{DR} in noise is a simplest test of the noise correction procedure. In other words, Z_{DR} should tend to zero at the periphery and outside of the radar echo. Similarly, the estimated ϱ_{hv} may not be accurately corrected for noise if its net value exhibits general increase or decrease at the periphery of the radar echo where SNR is low.

3. Algorithm for attenuation correction

a. Brief review of polarimetric techniques for attenuation correction at C band

First polarimetric technique for attenuation correction of Z and Z_{DR} was suggested by Bringi et al. (1990). According to this methodology, the biases of Z and Z_{DR} are estimated from simple formulas

$$\Delta Z = \alpha \Phi_{DP} \qquad (1)$$

$$\Delta Z_{DR} = \beta \Phi_{DP} \quad , \qquad (2)$$

where the coefficients α and β are supposed to be constant. The coefficient α is the ratio of specific attenuation A_h and specific differential phase K_{DP}, whereas the coefficient β is the ratio of specific differential attenuation A_{DP} and K_{DP}. Testud et al. (2000) proposed another correction algorithm for Z (the "ZPHI" rain-profiling algorithm) which also assumes a fixed coefficient α. Later on, Bringi et al. (2001) extended the ZPHI method to optimize the coefficients α and β by examining radial profile of Φ_{DP} and imposing constraint on the corrected value of Z_{DR} at the far side of attenuating rain cell. Most recent modification of the attenuation correction algorithm at C band presented by Vulpiani et al. (2008) attempts to take into account variability of the coefficients α and β by identifying the prevailing rain regime and adjusting them accordingly. Tabary et al. (2008) further advanced attenuation correction of Z_{DR} originally proposed by Smyth and Illingworth (1998) by taking into account that intrinsic value of Z_{DR} in the shadow of attenuating cell is a function of Z there. All mentioned attenuation techniques assume that the coefficients α and β are constant along the whole propagation path.

A different approach for attenuation correction was suggested by Ryzhkov et al. (2006, 2007), according to which the parameters α and β in the strong convective cells ("hotspots") along the propagation path may be very different from the rest of the path. In this study, we adopt such an approach after its slight modification.

b. Attenuation and differential attenuation in hotspots.

High variability of the coefficients α and β in strong convective cells is attributed to strong resonance scattering effects at C band which impact A_h, A_{DP}, and K_{DP} for raindrop sizes exceeding 5 mm (Ryzhkov and Zrnic 2005). The effects of resonance scattering at C band are illustrated in Fig. 3 – 5 where results of simulations of different radar variables from the measured drop size distributions in central Oklahoma are presented. Computations were made assuming that temperature of raindrops is 20°C and their shape depends on equivolume diameter as prescribed by Brandes et al. (2002).

Differential reflectivity Z_{DR} exhibits extreme variability for Z > 45 dBZ (Fig. 3). Very high Z_{DR} can be associated with relatively moderate values of Z. The scatterplots of A_h and A_{DP} versus K_{DP} are shown in Fig. 4. The degree of scatter is substantially reduced for Z_{DR} < 3 dB and the ratios A_h/K_{DP} and A_{DP}/K_{DP} are much more stable for lower Z_{DR}. Generally, both parameters $\alpha = A_h/K_{DP}$ and $\beta = A_{DP}/K_{DP}$ tend to increase with increasing Z_{DR}. This tendency is especially well pronounced for the ratio A_{DP}/K_{DP} (Fig. 5). The major conclusion from the simulations is that both α and β become extremely unstable for Z > 45 dBZ and Z_{DR} > 3 dB. Enhanced variability of α and β within hotspots was first noticed in the study of Carey et al. (2000).

In the suggested attenuation correction method, we assume that the ratios α and β are variable and unknown inside hotspots, whereas outside of them they are constant and equal to their average climatological values α_0 and β_0 which depend only on temperature for a given shape – size dependence for raindrops.

Identification of hotspots is a crucial component of the algorithm. They are detected using the 45 dBZ threshold for Z after preliminary correction of Z is performed using equation

$$\Delta Z = \alpha_0 \Phi_{DP} \quad . \quad (3)$$

It is also required that maximal value of Z_{DR} within the hotspot exceeds 3 dB after first iteration of the Z_{DR} correction for differential attenuation is completed according to the formula

$$\Delta Z_{DR} = \beta_0 \Phi_{DP} \quad . \quad (4)$$

Additional conditions include the requirement of $\varrho_{hv} > 0.7$ within hotspot, its sufficient length, and relatively large change of total differential phase Φ_{DP} (usually more than 10 – 30°) within the hotspot.

It is assumed that

$$\alpha = \alpha_0 + \Delta\alpha \quad (5)$$

and

$$\beta = \beta_0 + \Delta\beta \quad (6)$$

in the hotspot. If there are several hotspots detected along the ray, the parameters $\Delta\alpha$ and $\Delta\beta$ are assumed to be the same in all hotspots for a particular radial. However, these parameters are different for different radials.

According to the traditional ZPHI method (Testud et al. 2000), the old Hitschfeld – Bordan (1954) scheme is used with integral constraint based on the total span of differential phase within the range interval (r_0, r_m) containing radar echo

$$\int_{r_0}^{r_m} A_h(s)\,ds = \int_{r_0}^{r_m} \alpha K_{DP}(s)\,ds = \frac{\alpha}{2}\Delta\Phi_{DP}(r_0; r_m) \quad , \quad (7)$$

where

$$\Delta\Phi_{DP}(r_0; r_m) = \Phi_{DP}(r_m) - \Phi_{DP}(r_0) \quad . \quad (8)$$

Radial profile of $A_h(r)$ is estimated using attenuated radar reflectivity Z_a and $\Delta\Phi_{DP}$ using the formula

$$A_h(r) = \frac{[Z_a(r)]^b [10^{0.1 b \alpha_h \Delta\Phi_{DP}(r_0; r_m)} - 1]}{I(r_0; r_m) + [10^{0.1 b \alpha_h \Delta\Phi_{DP}(r_0; r_m)} - 1] I(r; r_m)} \quad , \quad (9)$$

where

$$I(r_0; r_m) = 0.46\, b \int_{r_0}^{r_m} [Z_a(s)]^b ds \quad (10)$$

and

$$I(r; r_m) = 0.46\, b \int_{r}^{r_m} [Z_a(s)]^b ds \quad . \quad (11)$$

The parameter b is an exponent in the relation $A_h = a Z^b$ and radar reflectivity factor in Eq (9) – (11) is expressed in linear units. Using (5), the constraint equation (7) can be rewritten as

$$\int_{r_0}^{r_m} A_h(s)\,ds = \alpha_0 \int_{r_0}^{r_m} K_{DP}(s)\,ds + \Delta\alpha \int_{HS} K_{DP}(s)\,ds = \frac{\alpha_0}{2}\Delta\Phi_{DP}(r_0;r_m) + \frac{\Delta\alpha}{2}\Delta\Phi_{DP}(HS) \quad , \qquad (12)$$

where integration in the second integral is performed over range gates within hotspots (HS) and $\Delta\Phi_{DP}(HS)$ stands for the Φ_{DP} increase within hotspots. Eq (12) stipulates that in the basic formula (9) for the traditional ZPHI method the term $\alpha\Delta\Phi_{DP}(r_0;r_m)$ should be replaced with the term $\alpha_0\Delta\Phi_{DP}(r_0;r_m) + \Delta\alpha\Delta\Phi_{DP}(HS)$. This means that two measured differential phase parameters, $\Delta\Phi_{DP}(r_0;r_m)$ and $\Delta\Phi_{DP}(HS)$, are used for constraining the procedure instead of one. As a result, radial profile of A_h becomes dependent on the value of $\Delta\alpha$. The appropriate factor $\Delta\alpha$ should be defined from the iterative process of incrementing $\Delta\alpha$ until certain condition is satisfied.

Two different conditions are tested in this study. One of them was used by Ryzhkov et al. (2006, 2007) and requires that

$$\int_{OHS} A_h(s,\Delta\alpha)\,ds = \frac{\alpha_0}{2}\Delta\Phi_{DP}(OHS) \quad , \qquad (13)$$

where integration is performed over the gates outside of hotspots (OHS) and

$$\Delta\Phi_{DP}(OHS) = \Delta\Phi_{DP}(r_0;r_m) - \Delta\Phi_{DP}(HS) \quad . \qquad (14)$$

Another one stipulates matching path-integrated rain rates obtained from corrected Z (which is a function of $\Delta\alpha$) and K_{DP}:

$$\int_{Rain} R(Z(\Delta\alpha))\,ds = \int_{Rain} R(K_{DP})\,ds \qquad (15)$$

In (15), rain rates are computed using formulas

$$R(Z) = 1.6910^{-2}10^{0.0717\,Z} \qquad (16)$$

and

$$R(K_{DP}) = 25.1\,|K_{DP}|^{0.777}\,\mathrm{sign}(K_{DP}) \qquad (17)$$

derived from C-band simulations utilizing measured DSDs in Oklahoma. In Eq (16) and (17), K_{DP} is expressed in deg/km and Z is in dBZ. Note that integration in Eq (15) is performed over the gates where $20 < R(Z(\Delta\alpha)) < 100$ mm/h and $\varrho_{hv} > 0.8$. One shouldn't expect good match between R(Z) and $R(K_{DP})$ in the areas of light rain where $R(K_{DP})$ is noisy or extremely heavy rain where R(Z) is usually higher than $R(K_{DP})$ (see more details in Section 5).

Finally, the corrected radar reflectivity factor is expressed as

$$Z(r) = Z_a(r) + 2\int_{r_0}^{r} A_h(s,\Delta\alpha)\,ds \quad , \qquad (18)$$

where Z and Z_a are in dBZ and $A_h(s,\Delta\alpha)$ is the profile of specific attenuation determined from Eq (9) with the parameter $\Delta\alpha$ satisfying conditions (13) or (15).

The procedure for the Z_{DR} attenuation correction is based on the original idea of Smyth and Illingworth (1998) according to which the measured value of Z_{DR} behind the attenuating cell is compared to what is expected in light rain in the shadow of this cell.

This idea was later modified by Bringi et al. (2001) and Tabary et al. (2008). In our algorithm, the attenuation-related bias in differential reflectivity is determined as

$$\Delta Z_{DR}(r) = 2\int \beta(s) K_{DP}(s) ds = \beta_0 \Phi_{DR}(r) + \Delta\beta \Delta\Phi_{DP}(HS) \ , \qquad (19)$$

where β_0 and $\Delta\beta$ are defined by (6). The parameter $\Delta\beta$ is estimated from equation

$$\Delta\beta = \frac{Z_{DR}^{(th)} - \min(Z_{DR}(r,\beta_0))}{\Delta\Phi_{DP}(HS)} \ , \qquad (20)$$

where

$$Z_{DR}(r,\beta_0) = Z_{DR}(r_0) + \beta_0 \Phi_{DP}(r) \ , \qquad (21)$$

$$Z_{DR}^{(th)} = -0.246 + 0.00615 Z_{min} + 0.000702 Z_{min}^2 \ , \qquad (22)$$

$\min(Z_{DR}(r,\beta_0))$ is a minimal value of Z_{DR} in the shadow of hotspot after first iteration of the Z_{DR} correction is made using formula (21), and Z_{min} is a value of corrected Z where minimum of Z_{DR} is observed.

The difference in our approach and the one of predecessors is that the coefficient β is modified in the hotspot only and not along the whole ray. Also, we suggest different formula for expected value of $Z_{DR}^{(th)}$ in the shadow of hotspot. The dependence (22) was derived from theoretical simulations illustrated in Fig. 3 for Z < 45 dBZ (grey line in Fig. 3).

4. Results of attenuation correction

Attenuation correction of Z and Z_{DR} was performed for all radar scans following every 6 minutes during the 2 hour period of observations after all data quality issues mentioned in section 2 have been addressed. We assume that the parameters α_0 and β_0 in the correction scheme are equal to 0.06 dB/deg and 0.01 dB/deg respectively which correspond to our theoretical estimates for C band and temperature 20°C.

The degree of attenuation at C band was really striking in this storm as can be seen from Fig. 6 where the fields of the measured Z (before correction for attenuation), corrected Z, differential phase Φ_{DP}, and Z obtained from S-band KLOT WSR-88D radar at 0149 UTC are displayed. The difference between measured and corrected Z at C band approaches 30 – 40 dB over extended areas of the storm. This is not surprising given the fact that Φ_{DP} exceeds 300° in large azimuthal sectors west and north of Sidpol.

The WSR-88D radar provides good reference for validating attenuation correction at C band because the S-band signal experiences much lower attenuation and the NEXRAD radar is located behind the squall line at 0149 UTC, hence the propagation path of the S-band microwave radiation through heavy rain is relatively short. It is evident that corrected Z at C band agrees very well with the one measured by WSR-88D within the squall line. However, if the attenuated C-band signal drops below noise level, as in the remote areas in the northern and western azimuthal sectors, then attenuation correction is not possible. The difference between corrected C-band Z and S-band Z in the stratiform part of the storm is caused by the height mismatch of the radar sampling volumes of the two radars at elevation 0.5° in this area. Indeed, the Sidpol radar samples the melting layer, whereas the corresponding radar resolution volume of WSR-88D is below the melting layer and, therefore, S-band Z is lower than C-band Z there.

Largest recoverable attenuation bias of more than 40 dB is estimated along the radial at the azimuth of 257.2° (line in Fig. 6) where Φ_{DP} as high as 602° has been

measured (Fig. 7a,b). This is a record value of differential phase ever reported. This is much higher than anything measured in the previous C-band studies in Europe and Australia. Amazingly, the polarimetric algorithm for attenuation correction is capable to reliably restore radar reflectivity in the situation when 99.99% of signal power is lost! Note that the Hitschfeld-Bordan attenuation correction scheme for a single-polarization radar experiences serious problems if attenuation barely reaches 10 dB or even lower.

Total differential attenuation along the same ray reaches 7 dB as Fig. 7c shows. This means that radar signal at vertical polarization is 7 dB stronger than at horizontal polarization and the range of signal detection would be longer if radar reflectivity at vertical polarization is measured. The advantage of measuring Z at vertical polarization in the situations of heavy attenuation was mentioned by Ryzhkov et al. (2006).

In addition to cross-check with S-band measurements, the quality of attenuation correction can be also attested via comparison of the rain rate profiles computed from corrected Z and K_{DP}. The $R(K_{DP})$ estimate does not depend on attenuation. Fig. 7d confirms that the R(Z) and $R(K_{DP})$ profiles along the radial at Az = 257.2° are in a good agreement if rain rate is less than 100 mm/h. As mentioned before, R(Z) usually exceeds $R(K_{DP})$ for rain rates higher than 100 mm/h.

The quality of Z_{DR} correction for differential attenuation is illustrated in Fig. 8 where the composite PPI plot of Z, Φ_{DP}, ϱ_{hv} and three fields of Z_{DR} is presented for the radar scan at 0124 UTC. Uncorrected differential reflectivity exhibits strong differential attenuation in the sectors of high Φ_{DP} where measured Z_{DR} drops below – 5 dB. Blank azimuthal sector in NW direction is caused by total attenuation of the radar signal. A simplistic correction procedure for differential attenuation based on the use of Eq (4) with $\beta_0 = 0.01$ dB/deg significantly improves Z_{DR} estimate but falls short of eliminating relatively large areas of negative Z_{DR} where differential attenuation is especially severe (Fig. 8c, marked as "simple correction"). This means that the parameter β should be increased quite significantly in certain azimuthal directions in order to fix the problem. A more advanced technique which automatically determines appropriate coefficient β in hotspots as described in Section 3 apparently does much better job (Fig. 8d, marked as "advanced correction") and ensures positive and more realistically looking Z_{DR}. There is no apparent artificial drop of Z_{DR} next to the blank sector with severe attenuation.

It is difficult to formulate a solid objective criterion for validating Z_{DR} correction similar to attenuation correction of Z. The algorithm robustness can be assessed taking into account the absence of negative corrected Z_{DR}, its general consistency with Z, and spatial / temporal continuity of the fields of corrected Z_{DR}. Detailed analysis of the images of corrected Z_{DR} for 2 hr period of observations indicates that the suggested algorithm for differential attenuation correction is quite robust and reliable. Occasional "bad radials" of corrected Z_{DR} take place but they are relatively rare and can be eliminated using considerations of azimuthal continuity.

Every radial of radar data containing hotspots is characterized by particular values of α and β which turn out to be highly variable. This agrees with theoretical predictions illustrated in Fig. 4 and 5. The scatterplots of parameters α and β versus maximal value of Z_{DR} in hotspots are shown in Fig. 9 a,b. These scatterplots summarize results for all radar scans at elevation 0.5° and indicate large variability of α and β in hotspots at C band. Most values of α are within the range between 0.05 and 0.20 dB/deg, whereas β varies mainly between 0.01 and 0.04 dB/deg. The estimates of α and β in this study are generally consistent with the previous findings of the authors for C-band observations in Alabama and Canada (Ryzhkov et al. 2007) and the estimates by Tabary et al. (2008) in France and Keranen and Yllasjarvi (2008) in Finland. Ryzhkov et al. (2007) reported median values of α between 0.08 and 0.22 dB/deg in rain and rain/ hail mixture, whereas Keranen and Yllasjarvi (2008) found most of them between 0.06 and 0.18 dB/deg. Tabary et al. (2008) and Keranen and Yllasjarvi (2008) claimed median values of β of 0.025 dB/deg and 0.035 dB/deg respectively in their investigations. Very high values of α

(up to 0.3 dB/deg) and β (exceeding 0.1 dB/deg) observed in this storm have also been reported in the referred studies.

Fig. 9 a,b show that both α and β tend to increase with increasing Z_{DR} in hotspots but such a tendency is clouded by large scatter. The scatterplot β versus α shows certain degree of correlation between the two parameters as expected in rain (Fig. 9c). Vulpiani et al. (2008) assumed that the ratio β/α is approximately constant and equal to 0.3. Although the average slope of the β – α scatterplot in Fig. 9c is close to 0.3, the excessive scatter testifies that the coefficients α and β are loosely connected.

The results illustrated in Fig. 6 - 9 are obtained using the attenuation algorithm with constraining condition (13). Utilizing alternate condition (15) generally yields very similar results. Nevertheless, applying condition (15) rather than (13) may reduce the number of apparent outliers in certain azimuthal sectors and vise versa. The difference between the attenuation correction schemes with the two conditions usually increases in the areas of very low ϱ_{hv} where both Φ_{DP} and K_{DP} can be erratic.

5. Rainfall estimation

Unaccounted attenuation severely restricts capability of a single-polarization radar to quantify precipitation at C and X bands. The extent of the problem is illustrated in Fig. 10 where the fields of rain rates estimated from the measured and corrected Z, K_{DP}, and WSR-88D are displayed for the radar scan at 0149 UTC. Eq (16) and (17) are used to convert Z and K_{DP} to rain rates at C band. Heavy underestimation of rain rate retrieved from uncorrected Z is obvious practically everywhere within the storm. In the areas west of the Sidpol radar where rain rates estimated from corrected C-band Z, K_{DP}, and S-band exceed 100 mm/h, the corresponding rain rates retrieved from the measured (uncorrected) C-band Z are less than 1 mm/h.

Fig. 11 illustrates the benefit of using an advanced version of the attenuation correction algorithm developed in this study instead of a simplistic one based on Eq (3) as far as rainfall estimation is concerned. The rain rate fields obtained from the two versions of attenuation correction technique are compared with the ones retrieved from K_{DP} and S-band Z in the regions of the heaviest rain north of the radar at 0149 UTC. It is evident that a simple attenuation algorithm (3) underestimates rain rates in the presence of hotspots (Fig. 11a) as comparison with panels (b), (c), and (d) in Fig. 11 shows. This further emphasizes necessity of utilizing the advanced version of the attenuation correction method. Note that after C-band Z is corrected for attenuation using the advanced correction technique the values of R(Z) are generally higher than the corresponding values of $R(K_{DP})$ in the center of heaviest rain cells. The scatterplot of estimated $R(K_{DP})$ versus R(Z) is shown in Fig. 12a. The agreement between R(Z) and $R(K_{DP})$ is generally good for R(Z) less than 80 – 100 mm/h but R(Z) is usually well above $R(K_{DP})$ in extremely intense rain. Theoretical simulations from the measured DSD in Oklahoma explain and confirm these observational findings (Fig. 12b).

The $R(K_{DP})$ relation yields reliable estimates of rain rate within the squall line which are in a good agreement with two other estimates (from corrected C-band Z and S-band Z). In the areas with rain intensity less than 5 mm/h, the $R(K_{DP})$ relation produces very noisy estimates of R which are not suitable for practical utilization (see Fig. 10). For this reason, we suggest to use the R(Z) relation in the regions of lighter rain (R(Z) < 10 mm/h) after Z is corrected for attenuation and switch to $R(K_{DP})$ if R(Z) exceeds 10 mm/h.

Several rain gages were identified in the area swept by the storm to validate radar rainfall estimation. Out of 17 gages within the area, only 8 produced reliable ground truth for such a validation. Moreover, merely 5 gages measured rain total in excess of 9 mm. The rest of the gages did not record any rain when the radar shows sizeable accumulation and, therefore, should be discarded as unreliable. The absence of dedicated and well calibrated gage network within the Sidpol coverage area does not allow performing

comprehensive verification of the radar rainfall measurements there. Nevertheless, even comparison with few gages has certain value for preliminary verification of the usefulness of C-band polarimetric measurements for quantitative precipitation estimation in the presence of severe attenuation.

The scatterplots of 2-hour radar-estimated rain accumulations versus gage totals for different radar relations and for corrected and uncorrected radar reflectivity are displayed in Fig. 13. The $R(K_{DP})$ relation demonstrates excellent performance for the gages with accumulations between 9 and 21 mm. This gives additional confidence in the $R(K_{DP})$ formula (17) for estimating moderate-to-heavy rain and for serving as a benchmark for attenuation correction described in Section 3 with the constraint condition (15) applied. However, the $R(K_{DP})$ relation is unreliable for lower rain rates. Indeed, the $R(K_{DP})$ formula yields negative rain total for the gage with accumulation of 3 mm. This is the major reason why the $R(K_{DP})$ relation should be substituted with R(Z) for rain rates lower than 10 mm/h according to our suggested rainfall estimation algorithm.

Combining $R(K_{DP})$ and R(Z) does not add much difference to the performance of radar rainfall algorithm for the gages with totals below 21 mm. As expected, the R(Z) relation underestimates rain total if Z is not corrected for attenuation. All radar algorithms underestimate maximal rain accumulation (47 mm) recorded by the gages. Underestimation for this particular gage is minimal if the R(Z) algorithm with corrected Z is utilized. One of the possible reasons for such an outlier is insufficient temporal sampling of rain (with 6 min update) by both Sidpol and WSR-88D radars. Indeed, as Fig. 14 shows, the onset of rain at this gage location might not be well captured by the radars. The radar-estimated rain rate jumps from 0 to more than 110 mm/h between two successive scans, hence the error due to poor temporal sampling can be significant.

Overall, rain totals obtained from corrected Z and K_{DP} which is not affected by attenuation show reasonable consistency which is indirect indication of validity of the attenuation correction scheme utilized. Although the comparison between rain rates obtained from radar and few gages does not provide enough evidence that the advanced attenuation correction scheme is better than the old simplistic one, rain total maps show that rain accumulations obtained by using R(Z) with advanced attenuation correction show better agreement with the rain accumulations from $R(K_{DP})$ than the ones with old correction. A more comprehensive study with larger number of gages and several storms is needed to further substantiate this claim.

6. Discussion

This investigation confirms the conclusions of several previous studies that the ratios A_h/K_{DP} and A_{DP}/K_{DP} can be anomalously high in hotspots and, therefore, the hotspots should be treated separately from the rest of the storm as far as attenuation correction is concerned. The question is: what causes anomalous attenuation / differential attenuation in hotspots? Tabary et al. (2008) attribute anomalously high differential attenuation (or the coefficient β) to the presence of wet hail mixed with rain. Ryzhkov et al. (2007) also found highest β of 0.12 dB/deg (accompanied by α = 0.20 dB/deg) in hailstorm which produced hail on the ground with sizes between 1.0 and 2.5 cm. The Chicago storm, however, didn't produce any hail at the surface. At least, no hail was mentioned in the Storm Report.

Storm vertical structure also does not reveal strong evidence of hail either on the ground or below the melting level. Typical vertical cross-sections of the corrected Z, Z_{DR}, as well as R(Z), $R(K_{DP})$, Φ_{DP}, and ϱ_{hv} are displayed in Fig. 15 at 0106 UTC for Az = ? Radar reflectivity after correction for attenuation barely exceeds 55 dBZ near the surface and at midlevels. The Z_{DR} column associated with an updraft is clearly seen at the leading edge of the storm centered at the distance of about 65 km from the radar. However, there is no evidence of noticeable depression of Z_{DR} and K_{DP} in the downdraft below the

melting level (at about 3 km height) in the core of a squall line. Such a depression is usually associated with descending hail. The areas of enhanced R(Z) and R(K_{DP}) below the melting layer are matched very well and maximal values of R(Z) and R(K_{DP}) do not differ significantly.

Interestingly, cross-correlation coefficient exhibits two well defined minima in the middle of high reflectivity cores. One of them is associated with heavy rain near the ground and another one, at the height between 5 and 7 km in the boundary between convective updraft and downdraft, is attributed to mixed-phase hydrometeors (supercooled large water drops mixed with partially melted graupel / hail). Note that radial steaks of low ϱ_{hv} are caused by strong vertical gradients of differential phase as explained by Ryzhkov (2007).

We hypothesize that high variability of the parameters α and β in hotspots at C band is attributed to the effects of resonance scattering by large raindrops which may or may not be associated with hail. In other words, anomalous attenuation and differential attenuation may happen in pure rain as well. However, the presence of hail usually increases supply of large drops which originate from melting hail. Recent theoretical study of melting hail by Khain et al. (2009) indicates that shedding of water from melting hailstones leads to enhancement in the concentration of very large drops with size of about 8 mm. In other words, dry hailstones of very different sizes end up with giant raindrops with approximately the same size. Such an enhancement in the number of very large drops may not be offset by their breakup if there is plenty of melting hail in the storm.

Finally, we would like to make a note on the quantitative use of Z_{DR} for polarimetric rainfall estimation at C band. Because Z_{DR} is so much affected by anomalously high differential attenuation in hotspots and negative biases of Z_{DR} of 5 – 10 dB are very common, we do not recommend utilizing Z_{DR} for quantitative precipitation estimation in convective storms at C band. This is too risky even if the algorithm for attenuation correction eliminates most of the Z_{DR} bias. Instead, specific differential phase K_{DP} (in combination with corrected Z) should be used more aggressively as opposed to S band where the R(Z, Z_{DR}) relations are quite efficient in convective rain (Giangrande and Ryzhkov 2008).

7. Conclusions

1. Extreme rain event in the Chicago metropolitan area has been examined with C-band polarimteric radar built by the EEC and owned by the University of Valparaiso. The focus of this study was primarily on attenuation correction of radar reflectivity Z and differential reflectivity Z_{DR} as well as rainfall estimation in the presence of severe attenuation.
2. The storm produced very high instantaneous rain rates and record attenuation of radar signal at C band. The measured differential phase Φ_{DP} which is proportional to path-integrated attenuation exceeded 600° in some azimuthal directions and the radar reflectivity Z has been successfully recovered after the signal was attenuated by more than 40 dB!
3. A new procedure for attenuation and differential attenuation correction has been developed and tested. The algorithm separates contributions of intense rain cells or "hotspots" (where Z > 45 dBZ and Z_{DR} approaches 3 dB) and the rest of signal propagation path to the path-integrated attenuation and differential attenuation. It is assumed that the ratios $\alpha = A_h/K_{DP}$ and $\beta = A_{DP}/K_{DP}$ are highly variable within "hotspots" and should be estimated independently for every radial using a certain set of constraints.
4. Statistical analysis of the parameters α and β shows that they can be anomalously high in hotspots consisting of pure rain which is not mixed with

hail. The presence of melting hail, however, may augment concentration of very large raindrops and further exaggerate effects of anomalous attenuation.

5. The algorithm for attenuation correction was validated using cross-checking with the S-band radar measurements which are relatively immune to attenuation and via consistency of the rain rate fields retrieved from corrected Z and K_{DP}.
6. The quality of rainfall estimation was verified using few rain gages in the area. The $R(K_{DP})$ relation showed good performance in moderate-to-heavy rain which underscores the benefit of using K_{DP} as a benchmark for robust attenuation correction. It is recommended to utilize the $R(K_{DP})$ relation in the areas of moderate-to-heavy rain (with $R > 10$ mm/h) and the R(Z) formula (after Z is corrected for attenuation) in lighter rain.

References

Brandes, E., G. Zhang, and J. Vivekanandan, 2002: Experiments in rainfall estimation with a polarimetric radar in a subtropical environment. *J. Appl. Meteorol.*, **41**, 674 – 685.

Bringi, V. N., and V. Chandrasekar, 2001: *Polarimetric Doppler Weather Radar: Principles and Applications*. Cambridge University Press, 636 pp.

Bringi, V. N., V. Chandrasekar, N. Balakrishnan, and D. S. Zrnic, 1990: An examination of propagation effects in rainfall on polarimetric variables at microwave frequencies. *J. Atmos. Oceanic Technol.*, **7**, 829-840.

Bringi, V. N., T. D. Keenan, and V. Chandrasekar, 2001: Correcting C-band radar reflectivity and differential reflectivity data for rain attenuation: A self-consistent method with constraints. *IEEE Trans. Geosci. Remote Sens.*, 39, 1906-1915.

Carey, L. D., S. A. Rutledge, D. A. Ahijevych, and T. D. Keenan, 2000: Correcting propagation effects in C-band polarimetric radar observations of tropical convection using differential propagation phase. *J. Appl. Meteor.*, **39**, 1405-1433.

Giangrande, S. E., and A. V. Ryzhkov, 2008: Estimation of rainfall based on the results of polarimetric echo classification. *J. Appl. Meteor.,* **47**, 2445 – 2462.

Gorgucci, E., G. Scarchilli, and V. Chandrasekar, 1992: Calibration of radars using polarimetric techniques. *IEEE Trans. Geosci. Remote Sens.*, **30**, 853 – 858.

Goddard., J., J. Tan, and M. Thurai, 1994: Technique for calibration of radars using differential phase. Electron. Lett., **30**, 166 – 167.

Hitschfeld, W., and J. Bordan, 1954: Errors inherent in the radar measurement of rainfall at attenuating wavelengths. *J. Meteor.*, **11**, 58 – 67.

Keranen, R., and J. Yllasjarvi, 2008: Estimates for polarimetric attenuation coefficients in rain using multi season statistics of polarimetric C-band radar data in midlatitudes, with a case comparison to S band. *Fifth European Conference on Radar in Meteorology and Hydrology. Helsinki, Finland, 30 Jun. – 4 Jul.*

Khain, A., A. Pokrovsky, D. Rosenfeld, U. Blahak, and A. Ryzhkov, 2009: Effects of aerosols on precipitation and hail production in a midlatitude storm as seen from simulations using spectral (bin) microphysics model. Submitted to *J. Atmos. Sci.*

Ryzhkov, A. V., and D. S. Zrnic, 2005: Radar polarimetry at S, C, and X bands comparative analysis and operational implications. *32nd International Conference on Radar Meteorology*, Albuquerque, NW, USA.

Ryzhkov, A. V., S. E. Giangrande, V. M. Melnikov, and T. J. Schuur, 2005: Calibration issues of dual-polarization radar measurements. *J. Atmos. Oceanic Technol.*, **22**, 1138-1155.

Ryzhkov, A. V., D. Hudak, and J. Scott, 2006: A new polarimetric scheme for attenuation correction at C band. *Fourth European Conference on Radar in Meteorology and Hydrology. Barcelona, Spain, 18 – 22 Sept.*, 29-32

Ryzhkov, A. V., 2007: The impact of beam broadening on the quality of radar polarimetric data. *J. Atmos. Oceanic Technol.*, **24**, 729-744.

Ryzhkov, A., P. Zhang, D. Hudak, J. Alford, M. Knight, and J. Conway, 2007: Validation of polarimetric methods for attenuation correction at C band. *33rd Conf. on Radar Meteorology*, Cairns, Australia, CD-ROM P11B.12

Smyth, T. J., and A. J. Illingworth, 1998: Correction for attenuation of radar reflectivity using polarization data. Quart. *J. Roy. Meteor. Soc.*, **124**, 2393-2415.

Tabary, P., G. Vulpiani, J. J. Gourley, A. J. Illingworth and O. Bousquet, 2008: Unusually large attenuation at C-band in Europe: How often does it happen? What is the origin? Can we correct for it? *Fifth European Conference on Radar in Meteorology and Hydrology. Helsinki, Finland, 30 Jun. – 4 Jul.*

Testud, J., E. Le Bouar, E. Obligis, and M. Ali-Mehenni, 2000: The rain profiling algorithm applied to polarimetric weather radar. *J. Atmos. Oceanic Technol.*, **17**, 332-456.

Vulpiani, G., P. Tabary, J.Parent du Chatelet, F. Marzano, 2008: Comparison of advanced radar polarimetric techniques for operational attenuation correction at C band. *J. Atmos. Ocianic Technol.*, **25**, 1118-1135.

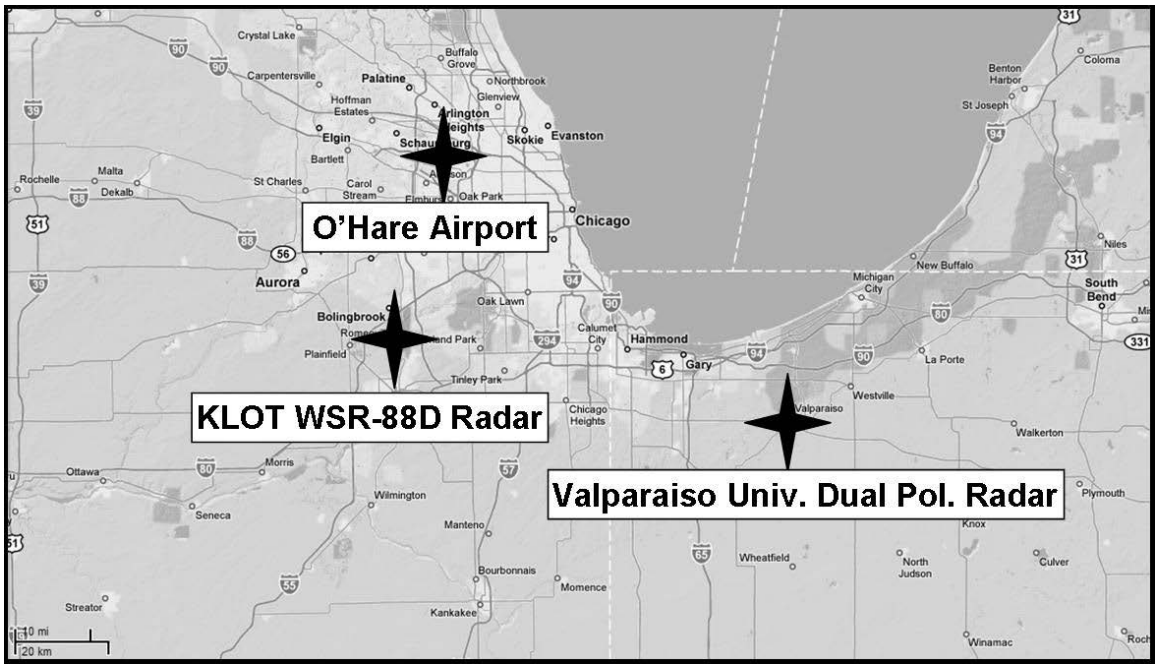

FIG. 1. Location of the C-band dual-polarization radar, S-band WSR-88D radar, and O'Hare International Airport.

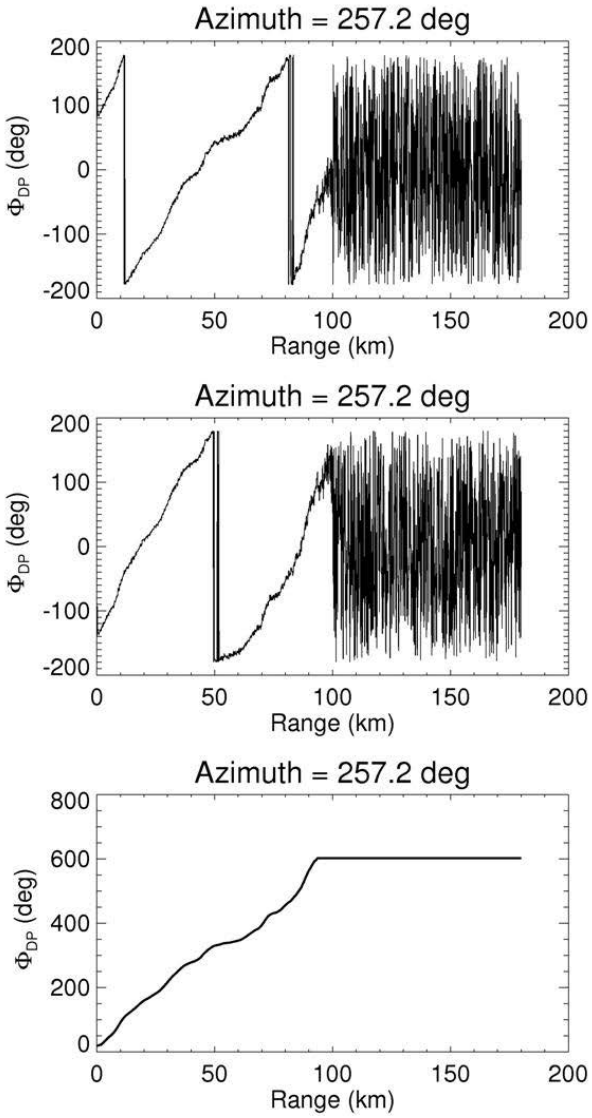

FIG. 2. Radial profiles of differential phase which was measured by the Sidpol radar (top panel), after downward phase shift (middle panel), and after editing, unfolding, and smoothing (bottom panel) at 0149 UTC on 2008/08/05 at Az = 257.2° and El = 0.5°.

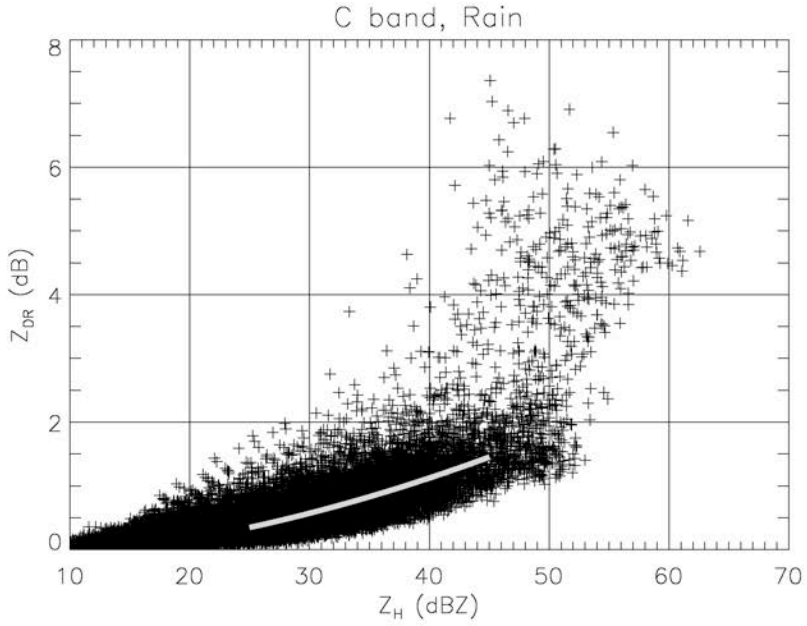

FIG. 3. Scatterplot of Z_{DR} versus Z in pure rain at C band. Z and Z_{DR} are computed from 25920 drop size distributions measured in central Oklahoma. Raindrop temperature is 20°C. The shape − size dependence of raindrops is assumed as in Brandes et al. (2002). Grey line indicates the dependence of median Z_{DR} on Z for $25 < Z < 45$ dBZ.

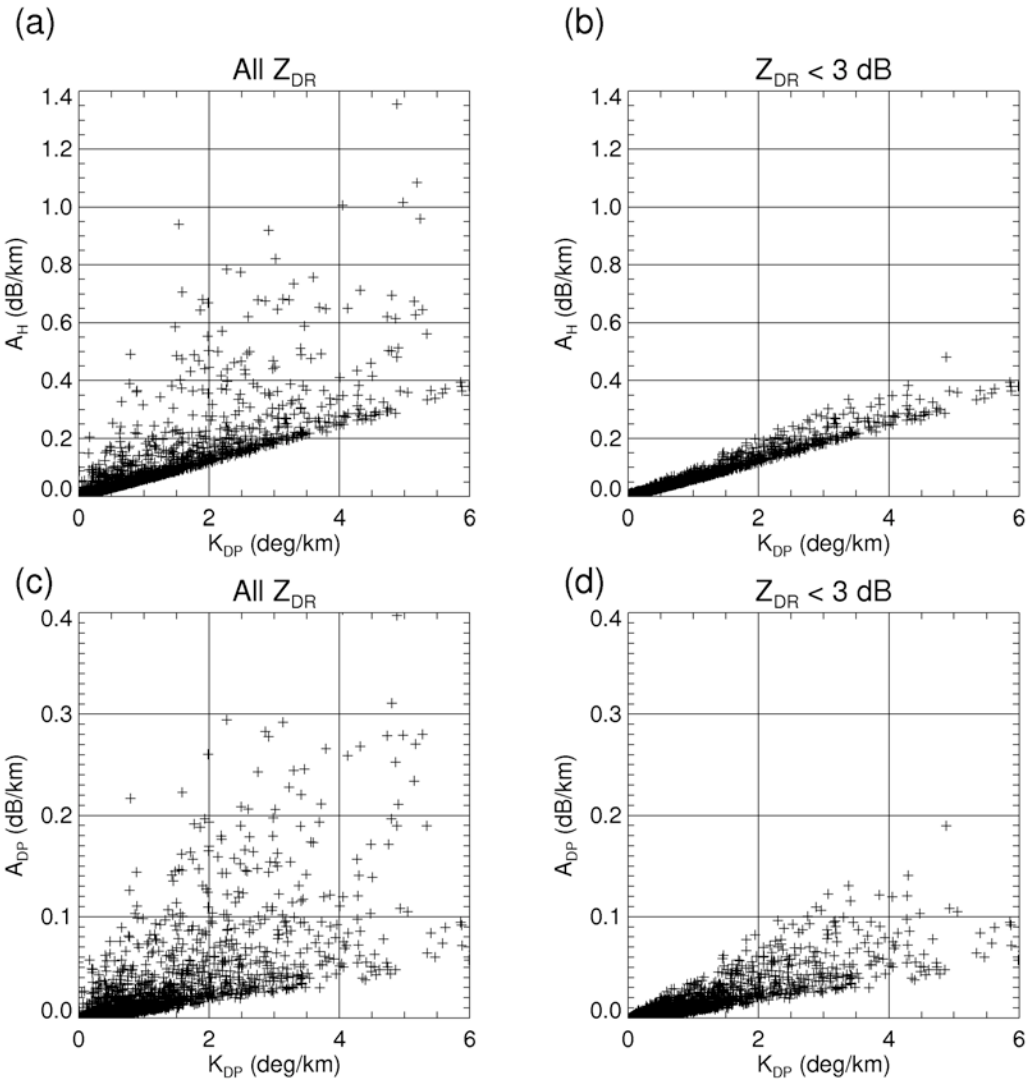

FIG. 4. Scatterplots of A_H and A_{DP} versus K_{DP} in pure rain at C band for all Z_{DR} (panels (a) and (c)) and for Z_{DR} < 3dB (panels (b) and (d)). Radar variables are computed from 25920 DSD measured in Oklahoma.

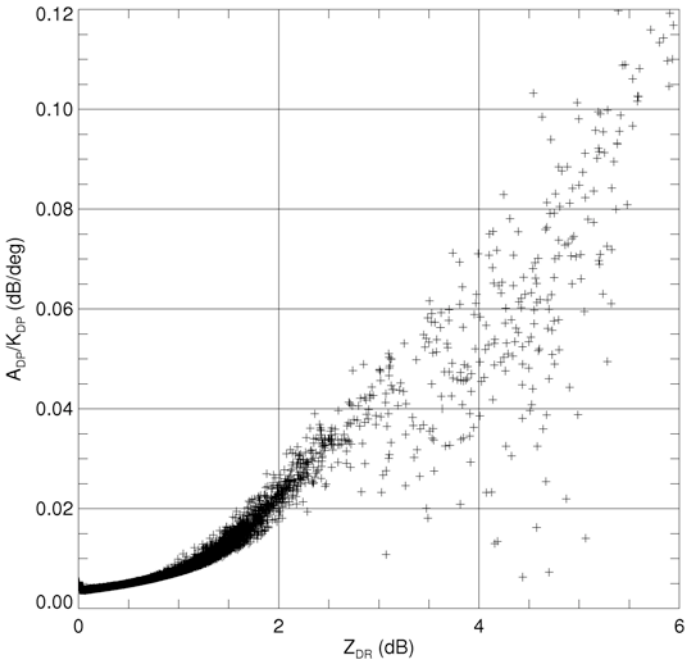

FIG. 5. Scatterplot of the ratio A_{DP}/K_{DP} versus Z_{DR} in pure rain at C band. Radar variables are computed from 25920 DSD measured in Oklahoma.

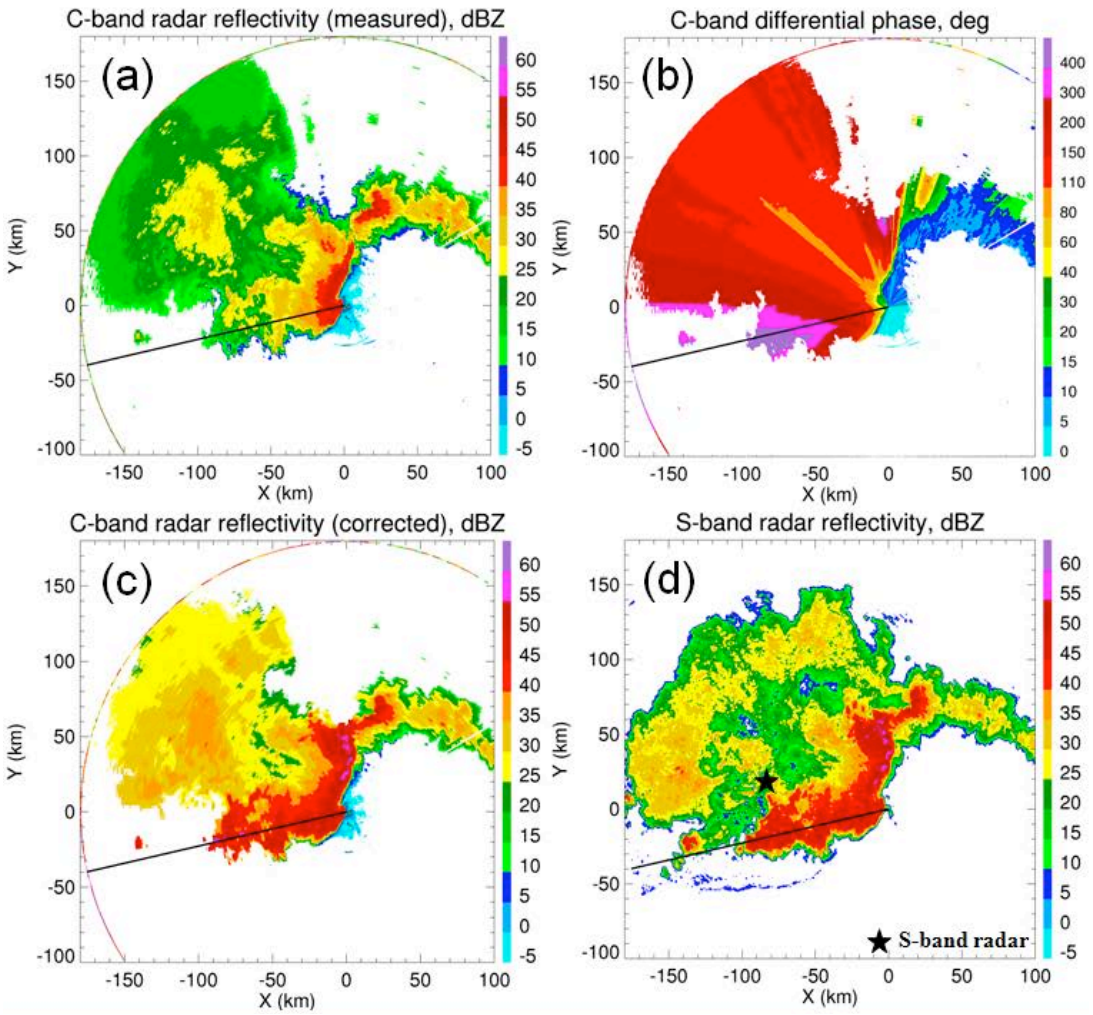

FIG. 6. Fields of measured and corrected Z at C band, Φ_{DP}, and Z measured by S-band radar (KLOT WSR-88D) at 0149 UTC on 2008/08/05. Antenna elevation is 0.5°. The Sidpol radar is situated at X = 0, Y = 0 km. A star marks location of the WSR-88D radar. Straight line indicates azimuth 257.2° (see Figs. 2 and 7).

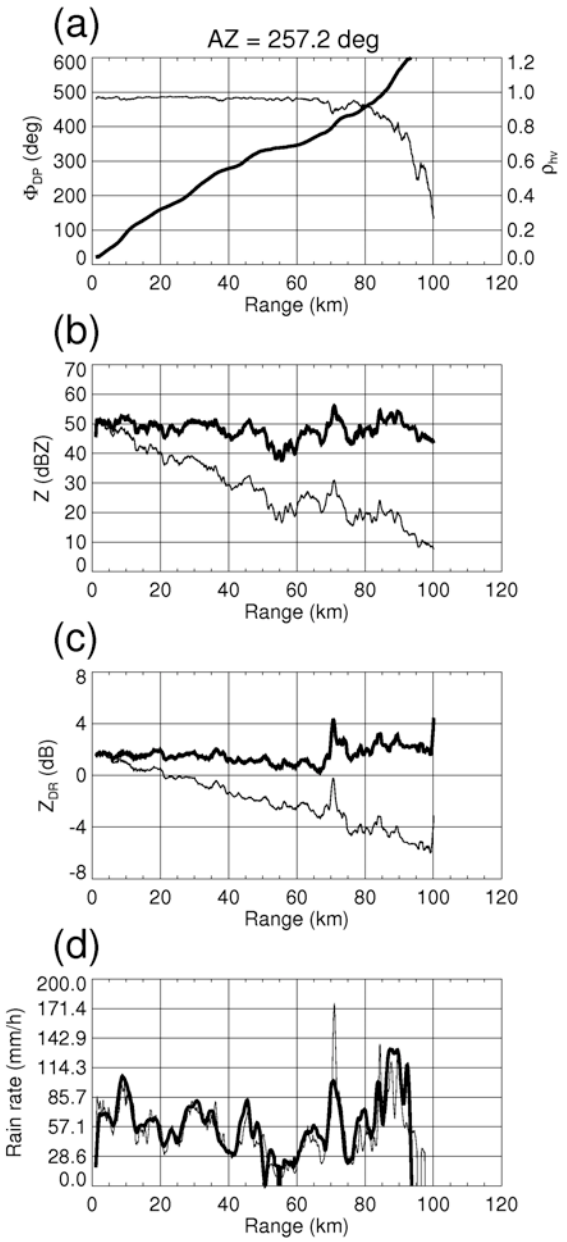

FIG. 7. Radial profiles of (a) Φ_{DP} (thick line) and ϱ_{hv} (thin line), (b) measured (thin line) and corrected (thick line) Z, (c) measured (thin line) and corrected (thick line) Z_{DR} and (d) R(Z) (thin line) after Z is corrected and $R(K_{DP})$ (thick line) at azimuth 257.2 deg at 0149 UTC on 2008/08/05. Attenuation correction of Z is performed using advanced algorithm with constraint condition (13).

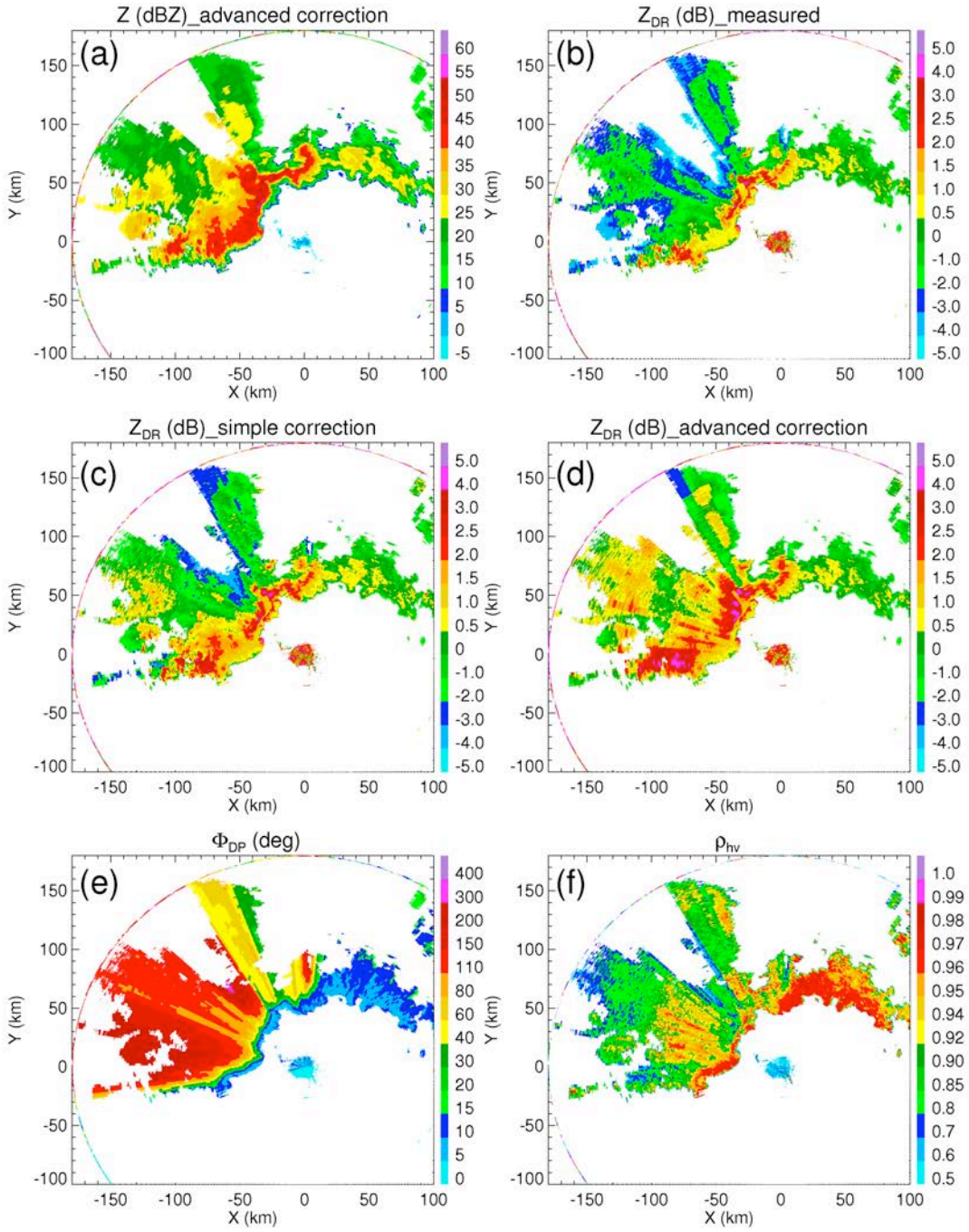

FIG. 8. Fields of corrected Z, measured and corrected Z_{DR}, Φ_{DP} and ϱ_{hv} at 0124 UTC on 2008/08/05. Antenna elevation is 0.5°

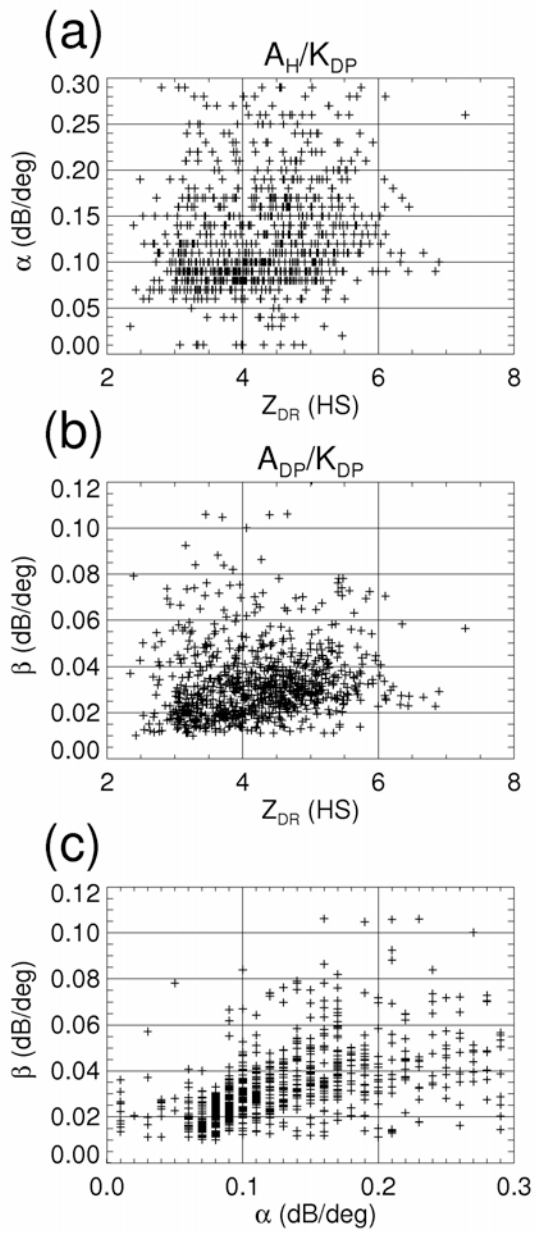

FIG. 9. Scatterplots of the measured parameters α and β versus maximal Z_{DR} in the "hotspot" at elevation 0.5 deg (panels a and b) and the scatterplot of β versus α in the "hotspots" (panel c).

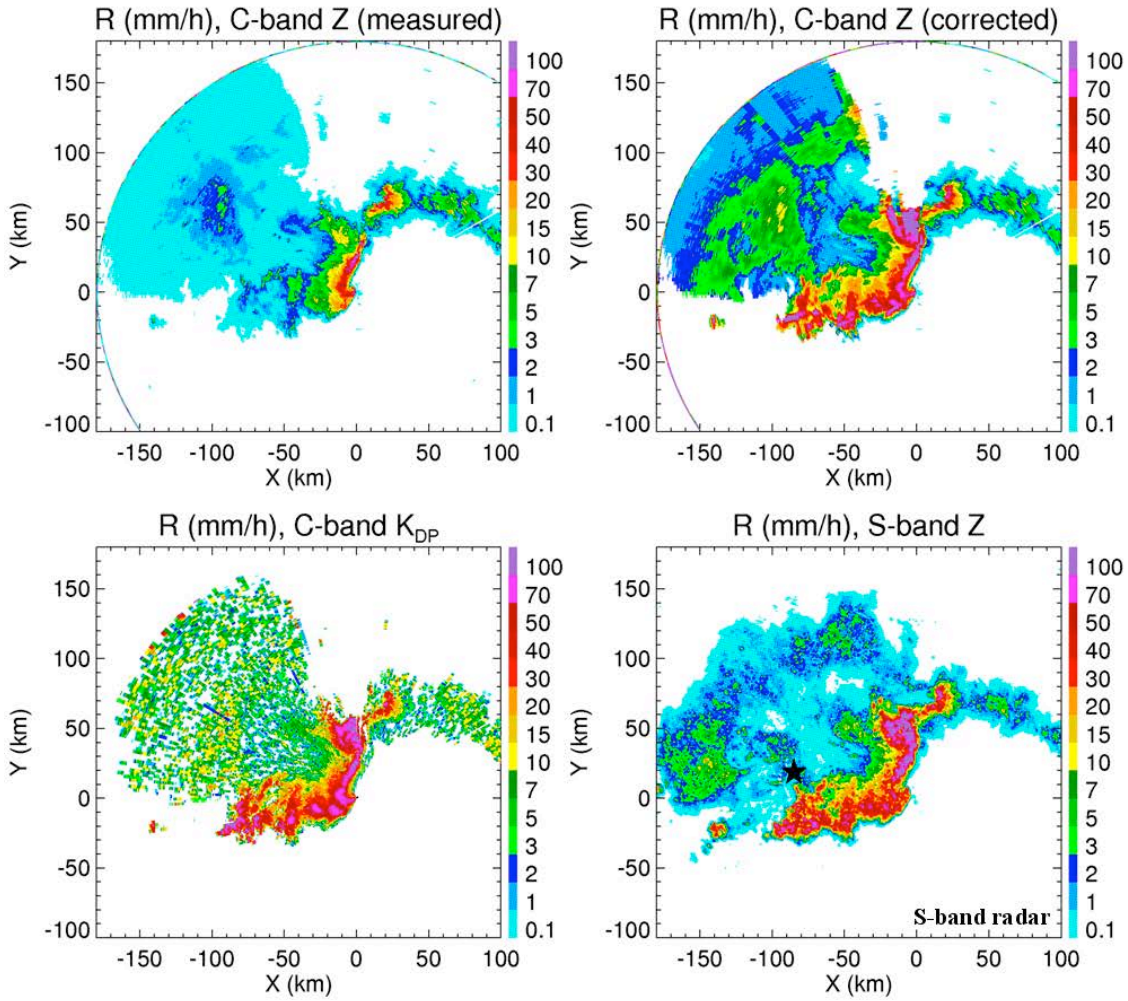

Fig. 10. Fields of rain rates obtained from measured and corrected Z at C band, K_{DP}, and S-band Z at 0149 UTC on 2008/08/05. A star indicates location of the WSR-88D radar.

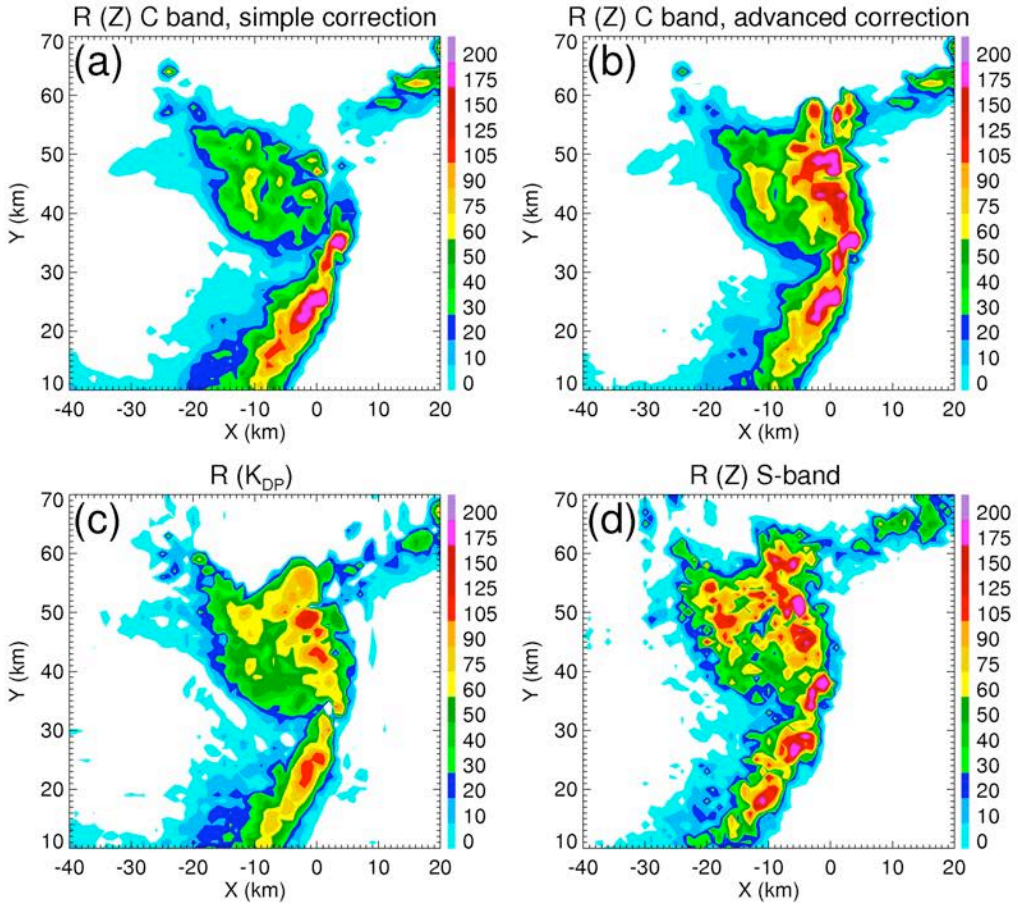

Fig. 11. Fields of rain rates obtained from C-band Z corrected using simple and advanced attenuation correction schemes, K_{DP}, and S-band Z at 0149 UTC on 2008/08/05.

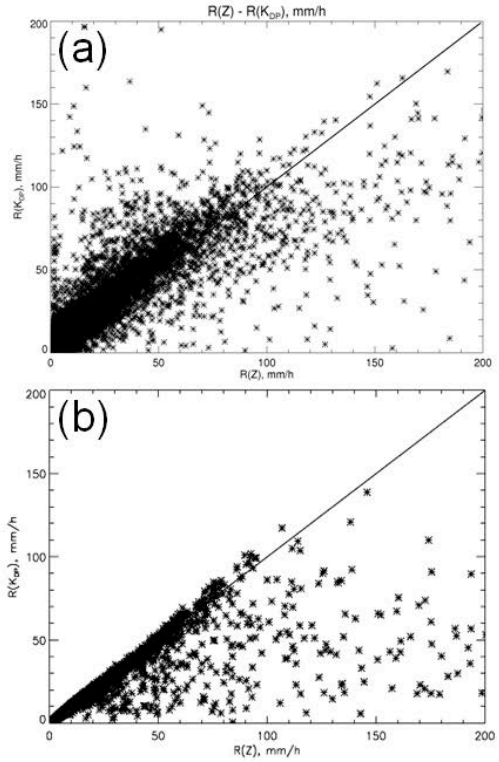

Fig. 12. Scatterplots of $R(K_{DP})$ versus R(Z) at C band from (a) observations and (b) simulations.

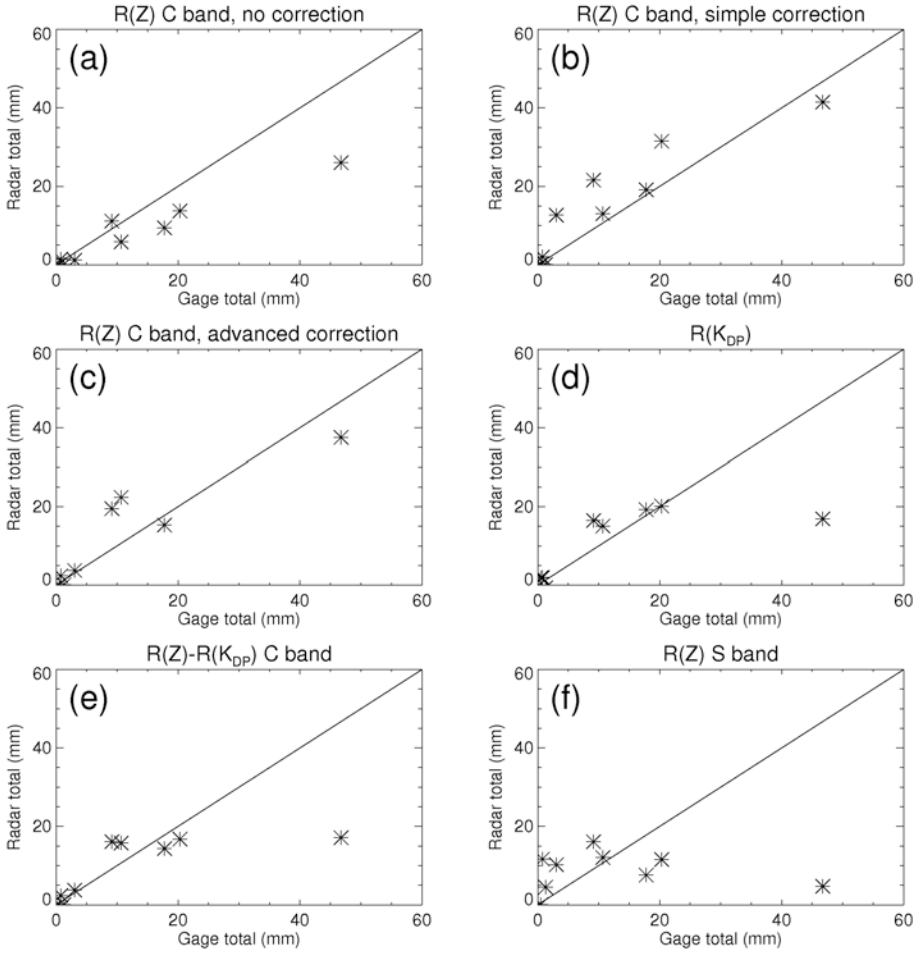

FIG. 13. Scatterplots of radar retrieved 2-hour rain totals versus gage 2-hour totals for the time interval from 00Z till 02Z on 08/05/2008 for different rainfall relations with corrected and uncorrected Z.

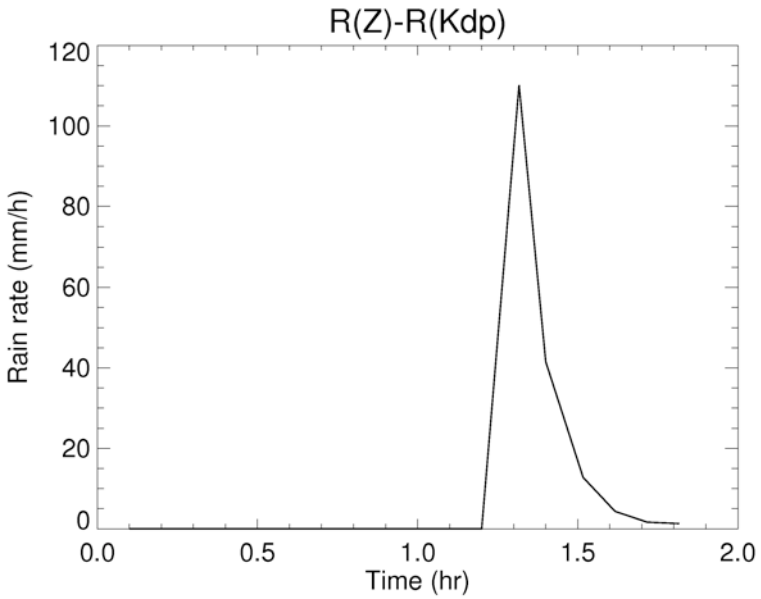

FIG. 14. Temporal dependence of rain rate measured by the radar at the location of the gage which recorded 47 mm of rain in 2 hours.

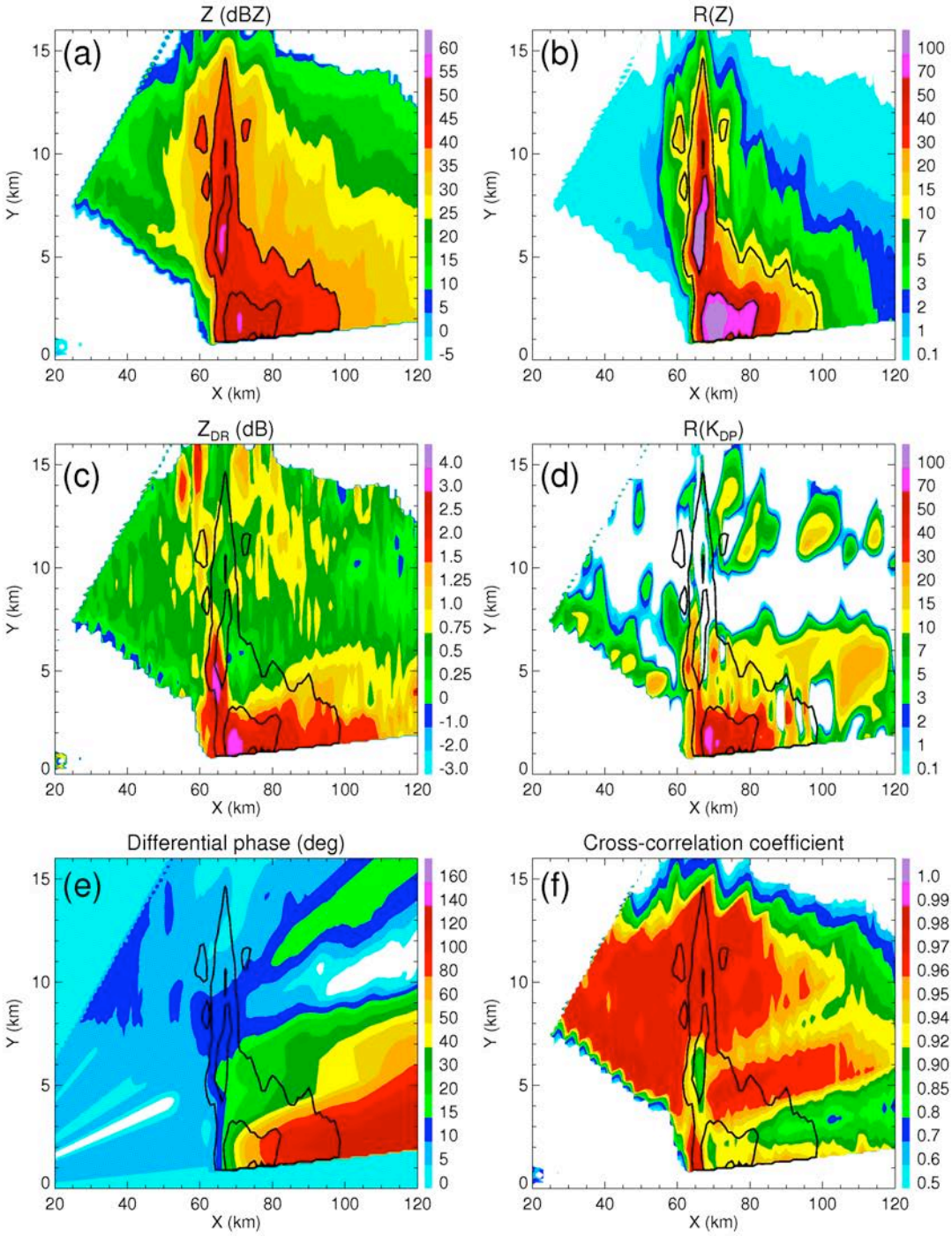

FIG. 15. Composite RHI plot of Z, R(Z), Z_{DR}, $R(K_{DP})$, Φ_{DP} and ϱ_{hv} at 0106 UTC on 2008/08/05.